

**Acurácia da ultrassonografia na detecção de metástases hepáticas de xenotransplantes
em camundongos nudes**

Accuracy of ultrasound for detecting liver metastasis xenografts in nude mice.

**Acuracia de la ultrasonografía en la detección de metástasis hepáticas de
xenotransplantes en ratones desnudos**

Recebido: 11/05/2019 | Revisado: 17/05/2019 | Aceito: 01/06/2019 | Publicado: 02/06/2019

Caroline Corrêa de Tullio Augusto Roque

ORCID: <https://orcid.org/0000-0002-7166-9049>

Omega Imagem veterinária, Brasil

E-mail: carolimagemvet@gmail.com

Eduardo Nóbrega Pereira Lima

ORCID: <https://orcid.org/0000-0003-1608-6964>

AC Camargo Cancer Center, Brasil

E-mail: eduardo.lima@accamargo.org.br

Rubens Chojniak

ORCID: <https://orcid.org/0000-0002-8096-252X>

AC Camargo Cancer Center, Brasil

E-mail: chojniak@accamargo.org.br

Bruno de Tullio Augusto Roque Lima

ORCID: : <https://orcid.org/0000-0001-5683-8839>

Qualittas, Brasil

E-mail: brunoroque.medvet@gmail.com

Tiago Goss dos Santos

ORCID: <https://orcid.org/0000-0001-6641-7413>

AC Camargo Cancer Center, Brasil

E-mail: tsantos@accamargo.org.br

Resumo

Os camundongos nudes são frequentemente utilizados em estudos relacionados à implantes ortotópicos. A ultrassonografia emergiu como um método viável na mensuração dos tumores implantados ortotopicamente. O objetivo desse estudo foi avaliar os achados ultrassonográficos de tumores hepáticos implantados em camundongos usando um transdutor

de 13 MHz e correlacionar esses achados com os achados macroscópicos e exames histológicos. As amostras tumorais de metástases hepáticas foram obtidas cirurgicamente de pacientes, e fragmentos de 1 mm³ foram implantados no parênquima hepático de 38 camundongos nudes. Os animais foram avaliados mensalmente através da ultrassonografia, até o momento da eutanásia dos mesmos. Dos 38 camundongos implantados, 11 desenvolveram o tumor. A ultrassonografia detectou lesões nodulares nos 11 animais macroscopicamente positivos e foi capaz de identificar as características dos tumores enxertados. Este trabalho demonstrou que a ultrassonografia é um método viável e não invasivo para avaliar o parênquima hepático de camundongos nudes, apresentando sensibilidade e especificidade de 100% na detecção e caracterização das lesões.

Palavras-chave: Ultrassom; camundongo nude; modelo pré-clínico; metástase hepática; xenoenxerto ortotópico.

Abstract

Nude mice are the usual animal model for studying orthotopically implanted human tumors, and ultrasound imaging has emerged as a viable method for measuring tumors implanted orthotopically. The aim of this study was to evaluate ultrasound findings of liver tumors implanted into mice using a 13-MHz transducer and to correlate these findings with gross pathology and histological examinations. Tumor samples from liver metastases were obtained surgically from patients, and 1-mm³ fragments were implanted into the liver parenchyma of 38 nude mice. Mice were imaged monthly by ultrasound until sacrifice. Of the 38 mice implanted with tumor fragments, 11 developed tumors. Ultrasound detected nodular lesions in the 11 macroscopically positive animals and was able to identify the features of the engrafted tumors. Ultrasound imaging is a viable and noninvasive method for evaluating the liver parenchyma of nude mice, and showed 100% sensitivity and specificity in detecting and characterizing lesions.

Keywords: Ultrasound; nude mice; preclinical model; liver metastasis; orthotopic xenograft.

Resumen

Se utilizan ratones nudes con frecuencia en estudios relacionados con los implantes ortotópicos. La ultrasonografía surgió como un método viable en la medición de los tumores implantados ortotópicamente. El objetivo de este estudio fue evaluar los hallazgos ultrasonográficos de tumores hepáticos implantados en ratones usando un transductor de 13 MHz y correlacionar esos hallazgos con los hallazgos macroscópicos y exámenes

histológicos. Las muestras tumorales de metástasis hepáticas fueron obtenidas quirúrgicamente de pacientes, y fragmentos de 1 mm³ se implantaron en el parénquima hepático de 38 ratones nudes. Los animales fueron evaluados mensualmente a través de la ecografía, hasta el momento de la eutanasia de los mismos. De los 38 ratones implantados, 11 desarrollaron el tumor. La ultrasonografía detectó lesiones nodulares en los 11 animales macroscópicamente positivos y fue capaz de identificar las características de los tumores injertados. Este trabajo demostró que la ultrasonografía es un método viable y no invasivo para evaluar el parénquima hepático de los ratones desnudos, presentando sensibilidad y especificidad del 100% en la detección y caracterización de las lesiones.

Palabras clave: ultrasonido; ratón desnudo; modelo preclínico; metástasis hepática; xenoinjerto ortotópico.

1. Introduction

Metastasis is the leading cause of cancer mortality. The liver is a frequent metastatic site for melanoma, colon, and breast cancer and therefore an important area of metastasis research. Patient-derived orthotopic xenograft (PDOX) in nude mice are the gold standard in preclinical cancer biology and tumor response to new drugs studies, and are uniquely suited for metastasis research. The use of preclinical models is essential in every aspect of translational cancer research, ranging from the biological understanding of the disease to the development of new treatments (Hidalgo, 2014). The rationale for developing patient-derived tumor xenograft (PDX) models is the expectation that these models will retain key characteristics of the donor tumor that will be maintained through successive mouse-to-mouse passages in vivo (Hidalgo, 2014). Nude mice make ideal hosts for tumor cell lines, because they have a mutation of the *Foxn1* gene leading to an athymic state, and thus exhibit depletion of CD4 and CD8 T cells and impaired T and B cell function (Oh, Hong, Lee, & Cho, 2017). Moreover, the orthotopic transplantation model is the most similar to human cancer in terms of histology, vascularity, gene expression, and the metastatic process. Thus, this model is able to develop metastasis and is superior to subcutaneous (ectopic) transplantation (Oh *et al.*, 2017; Kubota, 1994; Hoffman, 1999; Hoffman, 2015; Murakami *et al.*, 2016). However, the difficulty in tracking the progression of metastases through time due to the lack of noninvasive longitudinal imaging methods has limited their utility (Graham *et al.*, 2005).

Ultrasound imaging boasts excellent soft tissue contrast without the use of exogenous contrast agents or radiopharmaceuticals and offers considerably higher throughput than computed tomography (CT), magnetic resonance imaging (MRI), positron emission

tomography (PET), and bioluminescent imaging systems (Ayers *et al.*, 2010). In addition to being noninvasive and inexpensive, ultrasound does not require the use of ionizing radiation or special facilities, making it possible to perform serial examinations without injury or discomfort to the animal. Before the 1990s, ultrasound studies were limited primarily to larger animals, such as dogs, pigs, sheep, primates, and calves (Tanaka *et al.*, 1996). In 1995, researchers pioneered the use of high-frequency ultrasound imaging or ultrasound biomicroscopy (UBM) in translational research for analyzing early mouse mutant phenotypes in utero (Turnbull, Bloomfield, Foster, & Joyner, 1995). In 1999, researchers used high frequency (40 MHz) ultrasound imaging for monitoring apoptosis, and in 1996 another authors demonstrated the first application of UBM for studying mouse melanoma progression (Czarnota *et al.*, 1999; Turnbull *et al.*, 1996). Different studies demonstrated use of three-dimensional high-frequency ultrasound to track the growth of liver metastases produced by mesenteric vein injection of B16F1, PAP2, HT-29, and MDA-MB-435/HAL cells in experimental mouse models. In those studies, ultrasound imaging proved highly sensitive to small metastases with a minimum detection size of 0.22 mm (Cheung *et al.*, 2005; Graham *et al.*, 2005).

Despite all its advantages, the use of high-frequency ultrasound has been limited by its high costs. Thus, conventional ultrasound, which is routinely used in most diagnostic centers, emerges as a yet unexplored, alternative, noninvasive imaging method to detect liver nodules in nude mice. Also, there is currently a lack of comparative studies using conventional ultrasound to detect liver metastases in this animal model. Thus, this study aimed to assess the feasibility of using ultrasound to detect liver tumors implanted in immunodeficient mice, evaluating the sensitivity and specificity of ultrasound for detecting liver tumors implanted in immunodeficient mice with a 13-MHz linear transducer, and comparing gross pathology and histologic findings with ultrasound images. Given the lack of operators trained in performing the procedure in mice, no interobserver study was conducted. The implantation of tumor fragments from colorectal cancer patients directly into the liver of nude mice mimicked the clinical pattern of metastasis.

1. Materials and Methods

This is an experimental pilot study involving translational research. The nature of this research is qualitative, because the interpretation by the researcher and his opinions about the phenomenon under study was extremely important, corroborating with Pereira *et al.* (2018).

Animal model

This study employed 42 male and female Balb/c nude mice (Charles River), 8–16 week old and weighing approximately 20 g, and did not involve experimentation on genetically modified animals. Mice were kept in a specific pathogen-free (SPF) facility throughout the experimental period and tested periodically for specific pathogens. Mice were housed in microisolators controlled for temperature (22 °C) with a 12-h light/dark cycle and provided autoclaved water and irradiated rodent diet *ad libitum*. The use of animals in the research was approved by the Institutional Animal Care and Use Committee at AC Camargo Cancer Center (reference number 065/14A).

Patients and tumor sample collection

The patients selected for this prospective study fulfilled the following inclusion criteria: colorectal cancer with liver metastasis confirmed by core needle biopsy with indication for lateral segmentectomy. Patients signed the informed consent form and were operated on by the Abdominal Surgery team at A.C. Camargo Cancer Center, São Paulo, Brazil. Six patients were included in the study; all had received chemotherapy treatment. This study was approved by the Institutional Review Board at Antonio Prudente Foundation (number 1950/14). After collection, tumor samples from hepatic metastasis were transferred to plastic tubes containing culture medium (DMEM; Life Technologies, Carlsbad, CA, USA) supplemented with fetal bovine serum and transported to the animal facility in a closed vial inside a container packed with ice to keep temperature low. Mice were implanted with tumor fragments within 1 h after tumor collection.

Tumor inoculation

Tumor samples were cut into 1–2 mm³ pieces and each animal had one tumor fragment implanted into the left lobe of the liver parenchyma. Mice were anesthetized with an injection of ketamine/xylazine (100 mg/kg ketamine and 10 mg/kg xylazine). Following tumor implantation, mice received subcutaneous analgesia with tramadol (5 mg/kg) and were monitored under infrared light until complete recovery from anesthesia. Tumor growth was evaluated monthly and tumor burden was assessed when signs of apathy, weight loss, dehydration, and increased abdominal volume were observed. Mouse livers containing tumor xenografts were processed for histological and immunohistochemical analysis.

Ultrasound imaging

Ultrasound imaging data were collected using a MyLab™Gamma portable ultrasound system (Esaote Healthcare do Brasil, São Paulo, SP, Brazil). The linear transducer model SL1543, operates between 4 and 13 MHz with maximum of 50-mm focal depth for accurate evaluation of murine liver parenchyma. In this study, the transducer was operated at 13 MHz and mice were noninvasively imaged at about 30-day intervals based on the time to tumor progression of implanted tumors (43–294 days).

- 1) Mice were kept anesthetized with an intraperitoneal injection of 100 mg/kg ketamine and 10 mg/kg xylazine;
- 2) Mice were placed in a laminar flow hood over a sterile surgical dressing, positioned in dorsal recumbancy, parallel and to the right of the ultrasound system so that the right side of the body remained closer to the operator;
- 3) Ultrasound contact gel (~ 10 mm in height) was applied to the abdomen at room temperature (22 ± 2 °C);
- 4) The transducer was initially positioned parallel to the dorsal plane of the mouse with the ultrasound probe directed to the skull. Next, overview images of the liver parenchyma were acquired from left to right in the sagittal plane;
- 5) After finishing the scanning described above, the transducer was positioned transversely to the D-V axis with the probe directed to the right side of the animal and further imaging of the entire parenchyma was obtained in the cranio-caudal (C-C) orientation;
- 6) Images ranged in appearance from small areas, slightly hypoechoic (Fig. 1a) relative to the surrounding liver parenchyma, with indistinguishable borders identified as scar tissue, to solid, homogeneous hypoechoic mass (Fig. 1b; 1c) and solid, heterogeneous hypoechoic masses with distinct, irregular borders identified as tumors (Fig. 1d);
- 7) Mice were classified as positive (presence of one or more liver tumors) or negative (absence of nodular images) as assessed by ultrasound imaging. The number and location of xenograft tumors were not considered;
- 8) The length (cranio-caudal diameter along the longitudinal axis of the liver) and height (dorsal-ventral diameter along the longitudinal axis of the liver) of each xenograft tumor were measured to the nearest mm.

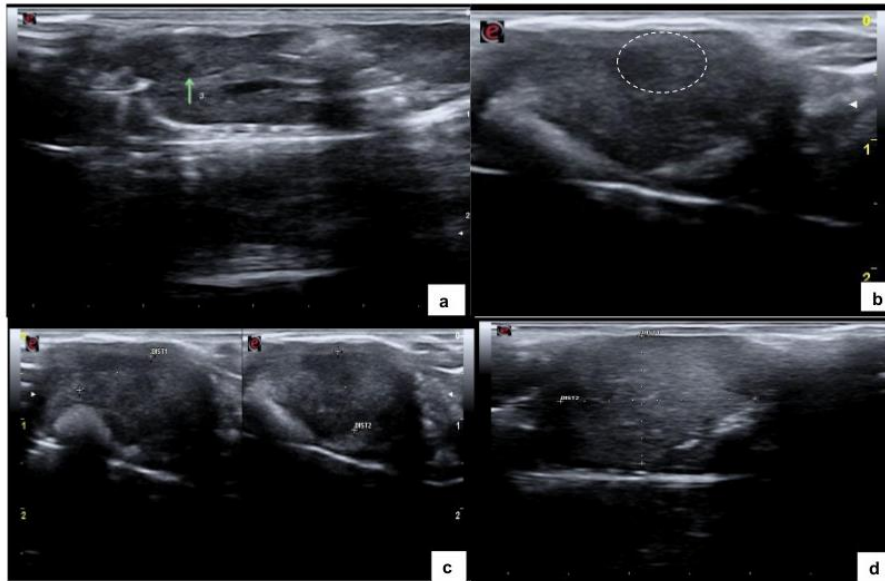


Fig. 1. (A) Ultrasound image of liver parenchyma showing a small, homogeneous hypoechoic nodule within the liver parenchyma measuring 1.2 mm in length along the longitudinal axis (green arrow). (B) Homogeneously hypoechoic nodule (dashed oval), distinct borders measuring 4.8mm. (C) Heterogeneously hypoechoic nodule measuring 12 mm × 8.2 mm (green arrow). (D) Heterogeneously hyperechoic nodule occupying a large portion of the liver parenchyma (dashed oval), measuring 17.1 mm in length along the longitudinal axis (diameter 2).

Euthanasia

Mice with liver tumors detected on ultrasound imaging, mice housed in the same microisolator cage as at least one tumor-bearing mouse diagnosed on ultrasound, mice with clinical signs of apathy or dehydration, and those housed for a period exceeding one year were euthanized. Mice were euthanized with an overdose of ketamine/xylazine sufficient to produce respiratory depression and death.

Histopathology

At necropsy, the livers were removed and assessed for macroscopically visible tumors and results compared with ultrasound findings. On gross pathology, a small whitish area identified as scar tissue was visualized at the site of implantation in livers that appeared as non-nodular, slightly hypoechoic areas on ultrasound images. All tumors appearing as solid masses on ultrasound images were also solid on gross pathology. Next, liver sections were stained by hematoxylin and eosin (H&E) and examined by two experienced pathologists (Drs. Maria Dirlei Begnani and Patrícia Peresi) for histologic confirmation of colorectal cancer.

Statistical Analysis

Data were analyzed using contingency tables to test for correlations between macroscopic findings and ultrasound imaging data.

3. Results

Population survival

Of the 42 mice implanted with colorectal tumor fragments, four died from complications of anesthesia induction related to refractory hypotension and hypothermia immediately after implantation of orthotopic xenografts, and 38 mice survived and were included in the study.

Tumors identified in the sample

Gross pathology and histologic sections revealed that 11 (28.9%) of the 38 mice developed liver tumors (Table 1).

Table 1. Contingency table of ultrasound and gross pathology findings.

			Gross pathology		Total
			Negative	Positive	
US detection	Negative	N	27	0	27
		% US detection	100.0%	0.0%	100.0%
		% gross pathology	100.0%	0.0%	71.1%
	Positive	N	0	11	11
		% US detection	0.0%	100.0%	100.0%
		% gross pathology	0.0%	100.0%	28.9%
Total		N	27	11	38
		% US detection	71.1%	28.9%	100.0%
		% gross pathology	100.0%	100.0%	100.0%

US: ultrasound

Gross pathology

Of the 38 living mice, only 11 (28.9%) exhibited one or more macroscopically visible liver tumors and 27 (71.1%) were negative for liver tumors on gross pathology (Table 1). On gross pathology, liver tumors appeared as either diffuse (Fig.2a), multifocal (Fig. 2 b), or solitary lesions at the site of implantation (Fig. 2c).

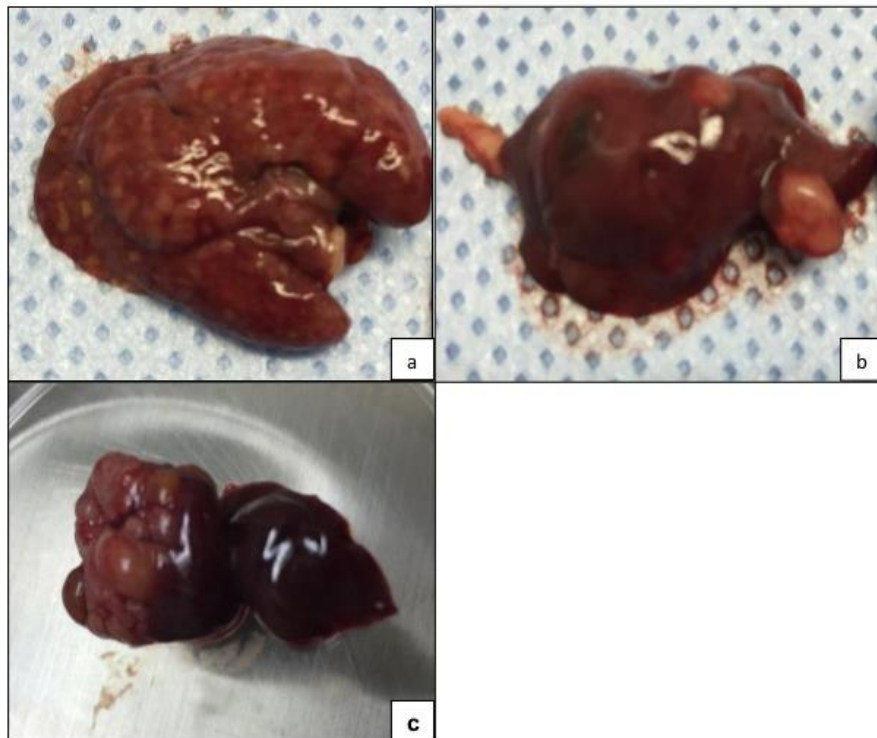


Fig. 2. Explanted gross specimens reveal morphologically distinct hepatic lesions, indicated by tissue discoloration: (A) diffuse, (B) multifocal, and (C) solitary lesions.

Histological findings

Of the 38 liver samples sent for H&E staining, 11 (28.9%) were positive for colorectal cancer as a result of tumor growth post-implantation and 27 (71.1%) were histologically negative for tumor cells (Table 1).

Ultrasonographic findings

Ultrasound imaging was obtained from 38 mice, of which 19 (50%) had a homogeneous and normoechoic liver parenchyma and no tumors on gross pathological examination and histologic sections (Fig. 3). In the remaining 19 mice (50%), at least one nodule measuring between 1.2 mm and 17.1 mm in diameter along its longitudinal axis was detected by ultrasound. Liver nodule appeared as:

- a) Small hypoechoic structure measuring <3 mm with homogeneous echotexture visualized in the left lobe of the liver in eight histologically negative mice and consistent with scar tissue. These findings, measuring up to 2.8 mm along the longitudinal axis (cranio-caudal diameter), showed no morphological evolution on serial ultrasound imaging and are consistent with scar tissue.

- b) Nodule measuring >3 mm visualized in 11 histologically positive mice, of which:
- eight appeared as hypoechoic images measuring >3 mm with slightly coarse echotexture and defined borders;
 - three appeared as predominantly hypoechoic images measuring >10 mm with heterogeneous echotexture and small, sparse pin-point hyperechoic areas (probably representing mineralization), and distinct irregular borders.

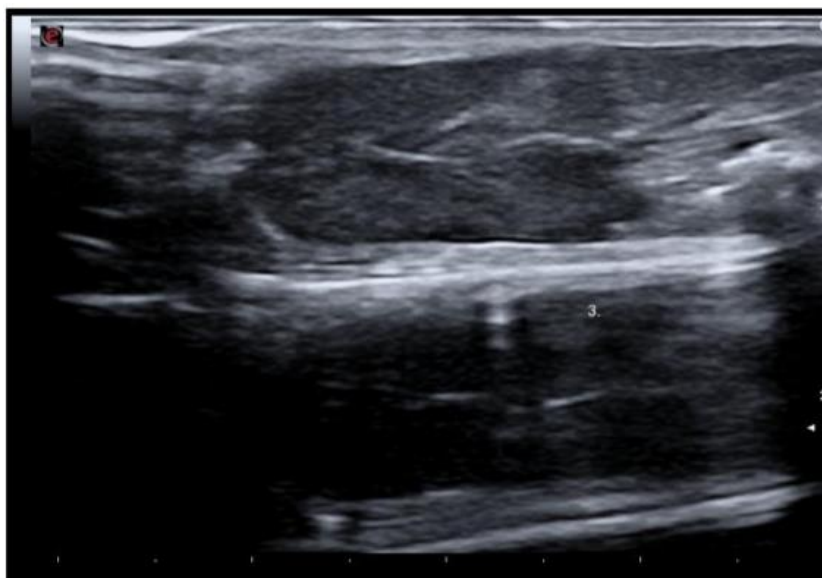


Fig. 3. Ultrasound image of a homogeneous and normoechoic liver parenchyma.

Dimensions

Ultrasound findings measuring up to 2.8 mm along the longitudinal axis (cranio-caudal diameter) consistent with scar tissue and without volume changes on serial ultrasound imaging were detected in eight mice, whereas solid masses measuring >3 mm with progressive growth were visualized in 11 mice.

The measurements for maximum tumor diameter of solitary tumors and multiple tumors within the same liver (mean: 6.97 mm, median: 4.90 mm) obtained from ultrasound images are listed in Table 2.

Table 2. Measurements for the longest tumor diameter obtained from ultrasound images.

Mouse	mm	Mouse	mm	Mouse	mm	Mouse	mm
1	1.3	6	2.4	11	5.0	16	12.8
2	1.4	7	2.6	12	10.5	17	14.2

3	1.4	8	2.8	13	10.9	18	14.2
4	1.5	9	3.1	14	12.0	19	17.1
5	2.2	10	4.9	15	12.3		

Tumor growth time

Tumor growth times after surgical implantation of patient-derived xenografts ranged from 43 to 294 days due to the heterogeneity of tumor fragments.

Accuracy

The ability of ultrasound to detect true positives among individuals with liver tumors was 100%.

The ability of ultrasound to identify true negatives among truly healthy mice was 100%. Of the 27 mice negative for colorectal cancer on gross pathological examination, 19 were identified as negative because no liver tumors were detected in ultrasound images, and eight mice with non-nodular, hypoechoic images measuring <3 mm with homogeneous echotexture and indistinguishable borders at the site of implantation were identified as negative for cancer by ultrasound imaging.

There was 100% agreement between positive cases detected by gross pathology and ultrasound imaging. The proportion of healthy mice (negative on gross pathology) among those negative on ultrasound was 100% (Table 1).

Clinical pathological characteristics

In this work, we aimed to establish orthotopic xenografts from six patients with metastatic colorectal cancer. The clinical pathological characteristics at the time of tumor implantation are shown in Table 3.

Table 3. Patient characteristics at the time of tumor implantation.

Patient number	Gender	Age at surgery	Primary diagnosis	Previous treatment
1	female	50	Colorectal carcinoma with mutated KRAS	1 st -FOLFOX 2 nd -FOLFOX + Bevacizumab 3 rd -FOLFIRI + Bevacizumab
2	male	67	Colorectal carcinoma wild-type KRAS	1 st -FOLFIRI + Cetuximab 2 nd -DEBIRI 3 rd -FOLFIRI + Avastin
3	male	68	Colorectal carcinoma and hepatocarcinoma	1 nd -FOLFOX + Bevacizumab 2 rd -FOLFIRI + Bevacizumab
4	male	41	Colorectal carcinoma wild-type KRAS	1 st -FLOX + Bevacizumab 2 nd -FOLFIRI
5	female	51	Colorectal carcinoma	1 st -FOLFOX + percutaneous RFA 2 nd -FOLFIRI + Bevacizumab
6	male	74	Colorectal carcinoma	1 st -FOLFOX

FOLFOX = 5-fluoracil + oxaliplatin; FOLFIRI = 5-fluoracil + irinotecan; FLOX = leucovorin + 5-fluoracil + oxaliplatin; DEBIRI = chemoembolization with irinotecan; RFA = radiofrequency ablation.

Success rate per patient sample

The number of mice per patient sample ranged from three to 10, and implantation success rates per tumor sample confirmed by gross pathology and histologic sections ranged from 0–100% (Table 4). This variation in success rates among patients was due to the genetic heterogeneity of implanted human tumors. Tumor fragments were obtained surgically from patients who had completed at least one chemotherapy cycle and had the highest rates of necrosis, fibrosis, calcifications, and inflammatory infiltrates.

Table 4. Number of mice per patient sample and respective tumor implantation success rates.

Patient	Animal	Implantation success rate (%) per patient	Ultrasound		Gross pathology	
			Positive	Negative	Positive	Negative
Patient 1	Mouse 1	100%	X		X	
	Mouse 2		X		X	
	Mouse 3		X		X	
	Mouse 4		X		X	
Patient 2	Mouse 1*	20%		X		X
	Mouse 2*			X		X
	Mouse 3			X		X
	Mouse 4		X		X	
	Mouse 5		X		X	
	Mouse 6			X		X
	Mouse 7			X		X
	Mouse 8*			X		X
	Mouse 9			X		X
	Mouse 10			X		X
Patient 3	Mouse 1	0%		X		X
	Mouse 2			X		X
	Mouse 3*			X		X
	Mouse 4			X		X
	Mouse 5*			X		X
	Mouse 6*			X		X
	Mouse 7*			X		X
Patient 4	Mouse 1	0%		X		X
	Mouse 2			X		X
	Mouse 3			X		X
	Mouse 4			X		X
	Mouse 5			X		X
Patient 5	Mouse 1*	56%		X		X
	Mouse 2			X		X
	Mouse 3			X		X
	Mouse 4			X		X
	Mouse 5		X		X	
	Mouse 6		X		X	
	Mouse 7		X		X	
	Mouse 8		X		X	
	Mouse 9		X		X	
Patient 6	Mouse 1	0%		X		X
	Mouse 2			X		X
	Mouse 3			X		X

*Mice with non-nodular areas at the implantation site on ultrasound images consistent with scar tissue.

4. Discussion and Conclusion

In this study, we used a PDOX model (implantation of tumor fragments from colorectal cancer patients directly into the liver of nude mice) to evaluate the accuracy of 13-MHz ultrasound for detecting liver tumors that mimic the clinical pattern of metastasis, as the tumor microenvironment at the site of implantation recapitulates the human tumor microenvironment (i.e., the liver). Comparison with gross pathological and histological

analyses indicates that ultrasound had 100% sensitivity and specificity in detecting and characterizing nodular lesions in murine liver parenchyma.

A study that used high-frequency (40 MHz) ultrasound to track the growth of murine liver metastases following orthotopic injection of tumor cell lines showed that ultrasound imaging was highly sensitive to metastasis (Graham *et al.*, 2005). Similarly, in our study ultrasound imaging showed 100% sensitivity and specificity to detect liver tumors. High frequency (40–60 MHz) transducers have been widely used in mouse studies due to their low penetration depth (range 1–2 cm) and high spatial resolution. Here, a 13-MHz transducer proved capable of mapping liver tumors in mice, contingent on the expertise of a well-trained and skilled operator. A report that a 10-MHz transducer could image only to a depth of 3–4 cm (Coatney, 2001).

The number of mice implanted with tumor fragments ranged from 3–10 per patient, with the viability of tumor cells affecting xenograft success. Tumor implants were generated based on the gross features of the sample by removing areas of friable tissue with a scalpel. However, tumor cells were not microscopically assessed for freezing damage immediately after surgical resection, which could have reduced the number of xenograft failures and increase tumor growth rates. This variation in tumor growth rates can be explained by tumor heterogeneity. In the context of tumor biology, metastatic tissue can exhibit varying degrees of cellularity, necrosis, and fibrosis according to histological type and molecular profile. In the current study, all mice housed in the same microisolator cage were killed and analyzed when the presence of a tumor was verified by ultrasound imaging in at least one animal. This was similar to the procedure adopted in 2005, who also killed the mice once suspected metastases were detected by ultrasound, to minimize false negatives and improve the accuracy of ultrasound (Graham *et al.*, 2005). Gross pathology revealed the presence of liver tumors in 11 mice, later confirmed in histologic sections. In eight mice, ultrasound findings measuring <3 mm in their largest dimension (cranio-caudal axis of the mouse) were identified by ultrasound as scar tissue at the site of implantation. Because no areas of scar tissue exceeded 3 mm in diameter on serial ultrasound imaging, a cut-off value of 3 mm for scar tissue can be tested in larger series. Liver tumors detected by ultrasound were serially followed to track tumor growth in all mice and were verified by gross pathology and histologic sections, indicating that ultrasound imaging was highly sensitive. In the remaining mice identified as tumor-free by ultrasound imaging, the liver parenchyma showed normal echotexture and echogenicity or appeared as homogeneously hypoechoic nodule at the site of implantation that showed no progression on serial ultrasound imaging, and these findings were later verified by

gross pathology and histologic sections. A single ultrasound examination is not capable of discriminating between scar tissue and early stage tumors because of their ultrasonographic features. Thus, ultrasound imaging only provides a highly accurate and sensitive means to assess liver tumors when mice are serially imaged.

The implantation of tumor fragments into the liver parenchyma of nude mice leads to hypotension intensifying the hypotensive effects of anesthesia. The four deaths during the experimental period were attributed to severe hypotension caused by the implantation of the tumor fragment into the liver parenchyma combined with the known hypotensive effects of the alpha-2 adrenergic agonist, xylazine.

This study had some limitations: there was no interobserver analysis, due to the unavailability of operators trained in performing the procedure in mice. In mice with multifocal lesion, a comparative analysis was not performed between each tumor detected by ultrasonography and gross pathology. In addition, all patients had completed at least one chemotherapy cycle before surgery, resulting in large areas of fibrotic and necrotic tissue in the tumor sample and adversely affecting the development of liver tumors in the mouse.

The need to develop models that can be used for studies on personalized treatments allowed various groups to lay the groundwork for experimental metastasis models over the last five decades. In the October 2014 issue of *Science*, in the section ‘On the Cover’, it was stated: “To make mice better mirrors of human cancer, researchers are building ‘avatars’ with the cancer of a particular patient,” underscoring the relevance of this type of mouse model in the current scenario (Frankel, 2014). Ultrasound imaging is a viable and noninvasive method for studying the liver parenchyma of nude mice. In this study, ultrasound showed 100% sensitivity and specificity in detecting and characterizing nodular lesions in murine liver parenchyma.

Conflict of Interest Statement: none.

References

Ayers GD, McKinley ET, Zhao P, et al. (2010). Volume of preclinical xenograft tumors is more accurately assessed by ultrasound imaging than manual caliper measurements. *J Ultrasound Med.* 29(6):891-901.

- Cheung AM, Brown AS, Hastie LA, et al. (2005). Three-dimensional ultrasound biomicroscopy for xenograft growth analysis. *Ultrasound Med Biol.* 31(6):865-870.
- Coatney RW. (2001). Ultrasound imaging: principles and applications in rodent research. *ILAR J.* 42(2):233-247.
- Czarnota GJ, Kolios MC, Abrahan J, et al. (1999). Ultrasound imaging of apoptosis: high-resolution non-invasive monitoring of programmed cell death in vitro, in situ and in vivo. *Br J Cancer.* 81(3):520-527.
- Frankel, J.C. (2014). The littlest patient. *Science.* 346(6205):24-27.
- Graham KC, Wirtzfeld LA, MacKenzie LT, et al. (2005). Three-dimensional high-frequency ultrasound imaging for longitudinal evaluation of liver metastases in preclinical models. *Cancer Res.* 65(12):5231-5237.
- Hidalgo M, Amant F, Biankin AV et al. (2014). Patient-derived xenograft models: an emerging platform for translational cancer research. *Cancer Discov.* 4(9):998-1013.
- Hoffman RM. (1999). Orthotopic metastatic mouse models for anticancer drug discovery and evaluation: a bridge to the clinic. *Invest New Drugs.* 17(4):343-359.
- Hoffman RM. (2015). Patient-derived orthotopic xenografts: better mimic of metastasis than subcutaneous xenografts. *Nat Rev Cancer.* 15(8):451-452.
- Kubota T. (1994). Metastatic models of human cancer xenografted in the nude mouse: the importance of orthotopic transplantation. *J Cell Biochem.* 56(1):4-8.
- Murakami T, Zhang Y, Wang X, et al. (2016). Orthotopic implantation of intact tumor tissue leads to metastasis of OCUM-2MD3 human gastric cancer in nude mice visualized in real time by intravital fluorescence imaging. *Anticancer Res.* 36(5):2125-2130.
- Oh, B.Y.; Hong, H.K., Lee, W.Y. & Cho, Y.B. (2017). Animal models of colorectal cancer with liver metastasis. *Cancer Lett.* 387:114-120.

Pereira, A.S.; Shitsuka, D.M.; Parreira, F.J. & Shitsuka, R. (2018). *Metodologia da pesquisa científica*. [e-book]. Ed. UAB/NTE/UFSM, Santa Maria/RS. Available from:
http://repositorio.ufsm.br/bitstream/handle/1/15824/Lic_Computacao_Metodologia-Pesquisa-Cientifica.pdf?sequence=1

Tanaka N, Dalton N, Mao L, et al. (1996). Transthoracic echocardiography in models of cardiac disease in the mouse. *Circulation*. 94(5):1109-1117.

Turnbull, D.H., Bloomfield, T.S., Foster, F.S. & Joyner, A.L. (1995). Ultrasound backscatter microscope analysis of early mouse embryonic brain development. *Proc Natl Acad Sci*. 92:2239-2243.

Turnbull DH, Ramsay JA, Shivji GS, et al. (1996). Ultrasound backscatter microscope analysis of mouse melanoma progression. *Ultrasound Med Biol*. 22(7):845-853.

Porcentagem de contribuição de cada autor no manuscrito

Caroline Corrêa de Tullio Augusto Roque – 30%

Eduardo Nóbrega Pereira Lima – 20%

Rubens Chojniak – 10 %

Bruno de Tullio Augusto Roque Lima – 30%

Tiago Goss dos Santos – 10%